


TanDEM-X elevation model data for canopy height and aboveground biomass retrieval in a tropical peat swamp forest

Michael Schlund, Felicitas von Poncet, Steffen Kuntz, Hans-Dieter Viktor Boehm, Dirk H. Hoekman & Christiane Schmullius

To cite this article: Michael Schlund, Felicitas von Poncet, Steffen Kuntz, Hans-Dieter Viktor Boehm, Dirk H. Hoekman & Christiane Schmullius (2016) TanDEM-X elevation model data for canopy height and aboveground biomass retrieval in a tropical peat swamp forest, International Journal of Remote Sensing, 37:21, 5021-5044, DOI: [10.1080/01431161.2016.1226001](https://doi.org/10.1080/01431161.2016.1226001)

To link to this article: <http://dx.doi.org/10.1080/01431161.2016.1226001>

 Published online: 23 Sep 2016.

 Submit your article to this journal [↗](#)

 Article views: 27

 View related articles [↗](#)

 View Crossmark data [↗](#)

TanDEM-X elevation model data for canopy height and aboveground biomass retrieval in a tropical peat swamp forest

Michael Schlund^{a*}, Felicitas von Poncet^b, Steffen Kuntz^b, Hans-Dieter Viktor Boehm^c, Dirk H. Hoekman^d and Christiane Schmullius^a

^aDepartment of Earth Observation, Friedrich-Schiller-University Jena, Jena, Germany; ^bAirbus Defence and Space, Immenstaad, Germany; ^cKalteng Consultants, Hoehenkirchen, Germany; ^dDepartment of Environmental Sciences, Wageningen University, Wageningen, The Netherlands

ABSTRACT

It was demonstrated in the past that radar data is useful to estimate aboveground biomass due to their interferometric capability. Therefore, the potential of a globally available TanDEM-X digital elevation model (DEM) was investigated for aboveground biomass estimation via canopy height models (CHMs) in a tropical peat swamp forest. However, CHMs based on X-band interferometers usually require external terrain models. High accurate terrain models are not available on global scale. Therefore, an approach exclusively based on TanDEM-X and the decrease of accuracy compared to an approach utilizing a high accurate terrain model is assessed. In addition, the potential of X-band interferometric heights in tropical forests needs to be evaluated. Therefore, two CHMs were derived from an intermediate TanDEM-X DEM (iDEM; as a precursor for WorldDEMTM) alone and in combination with lidar measurements used as terrain model. The analysis showed high accuracies (root mean square error [RMSE] = 5 m) for CHMs based on iDEM and reliable estimation of aboveground biomass. The iDEM CHM, exclusively based on TanDEM-X, achieved a poor R^2 of 0.2, nonetheless resulted in a cross-validated RMSE of 54 t ha⁻¹ (16%). The low R^2 suggested that the X-band height alone was not sufficient to estimate an accurate CHM, and thus the need for external terrain models was confirmed. A CHM retrieved from the difference of iDEM and an accurate lidar terrain model achieved a considerably higher correlation with aboveground biomass ($R^2 = 0.68$) and low cross-validated RMSE of 24.5 t ha⁻¹ (7.5%). This was higher or comparable to other aboveground biomass estimations in tropical peat swamp forests. The potential of X-band interferometric heights for CHM and biomass estimation was thus confirmed in tropical forest in addition to existing knowledge in boreal forests.

ARTICLE HISTORY

Received 6 January 2016
Accepted 8 August 2016

CONTACT Michael Schlund  michael.schlund@esa.int  Department of Earth Observation, Friedrich-Schiller-University Jena, Jena 07743, Germany

*Present address: European Space Research and Technology Centre (ESTEC), European Space Agency, Keplerlaan 1, 2200 AG Noordwijk, The Netherlands

© 2016 Informa UK Limited, trading as Taylor & Francis Group

1. Introduction

It is a prerequisite to estimate the aboveground biomass and its change over time to implement programmes, such as reducing emissions from deforestation and degradation (REDD+), where the reduction of carbon emission from deforestation and degradation and the enhancement of carbon stocks are incentivized. This could support climate change mitigation (Van der Werf et al. 2009; Gibbs et al. 2007; Olander et al. 2008). Tropical peat swamp forests and their soils play a significant role in the global carbon cycle because their carbon emissions equal one-fourth of total emissions from tropical forests despite their relatively small extent compared to the overall tropical forests (Page et al. 2002; Page, Rieley, and Banks 2011; Van der Werf et al. 2009; Lawson et al. 2015).

Estimating forest canopy height and subsequently biomass is considered high potential for large scale biomass estimations (Chavez et al. 2005; Koch 2010; Lefsky et al. 2002; Saatchi et al. 2011; Asner et al. 2009). A frequently used method is to produce a digital surface model (DSM) and by subtracting a digital terrain model (DTM) deriving a canopy height model (CHM). The CHM represents the vegetation height as well as the canopy surface, whereas the canopy surface represents the crown topography, which can be used, e.g. for single tree detection (Koch, Heyder, and Weinacker 2006). The vegetation height is frequently used to estimate the biomass in combination with field measured data, whereas the capability of airborne as well as space borne lidar was demonstrated (Boehm, Liesenberg, and Limin 2013; St-Onge, Hu, and Vega 2008; Dandois and Ellis 2013; Simard et al. 2011; Lefsky et al. 2005; Rosette, North, and Suárez 2008; Drake et al. 2002).

The Geoscience Laser Altimeter System (GLAS) on board of the ice, cloud, and land elevation satellite (ICESat) was a space borne lidar, which was used to extract vegetation height profiles from the laser signal estimating forest height accurately (Lefsky et al. 2005; Rosette, North, and Suárez 2008; Simard et al. 2011). ICESat acquired data not continuously but on ca. 65 m diameter footprints with a distance of 170 m along track and in the order of kilometres across track (Abdalati et al. 2010; Simard et al. 2011). Consequently, spatial sampling schemes are required for this space borne system to achieve continuous mapping results (Simard et al. 2011). The estimated canopy height from ICESat GLAS was further utilized with external data to estimate aboveground biomass on pan-tropical scale (Baccini et al. 2008; Saatchi et al. 2011). Today, lidar campaigns are mostly airborne, especially after the failure and retirement of ICESat GLAS, and thus lidar campaigns are cost-intensive compared to space borne systems (Köhl et al. 2011; Koch 2010). Subsequently, aboveground biomass estimations via airborne lidar sensors are applicable mainly for small spatial coverage or should be integrated in sampling schemes for large area applications (Asner et al. 2009).

For instance, optical as well as synthetic aperture radar (SAR) space borne sensors are suitable to derive digital elevation models (DEMs) on large areas consistently, allowing continuous canopy height estimation. However, only SAR sensors can acquire consistent data over tropical forests because of their weather and day/night independence. The potential of interferometric SAR (InSAR) for canopy height and aboveground biomass estimation has long been recognized. The method is based on the assumption that short wavelength SAR will penetrate marginally into the canopy. Thus, the resulting DEM can be considered to be a surface model (DSM). Shuttle Radar Topography Mission (SRTM) C-

and X-band were frequently used to estimate canopy height and biomass in combination with an external DTM (Sexton et al. 2009; Solberg et al. 2010; Weydahl et al. 2007). Kelldorfer et al. (2004) suggested a minimum mapping unit of 1.8 ha in order to yield stable estimates of SRTM height.

The TanDEM-X mission aims to create a global DEM with high resolution (12 m) on basis of interferometric SAR exploitation (Krieger et al. 2007). The accuracy of TanDEM-X to create a CHM with external lidar terrain model and the error sources were assessed in boreal forests, where the X-band and lidar surface heights difference ranged between 1.3 and 1.5 m (Sadeghi, Leblon, and Simard 2016). DEMs derived from TanDEM-X InSAR dataset were used to estimate canopy height and biomass of boreal forests resulting in a relative error of 43% on plot level and 19% on stand level (Solberg et al. 2013; Rahlf et al. 2014; Solberg et al. 2014). Forest attributes, such as forest height, basal area and volume were estimated with a CHM based on TanDEM-X as surface and lidar as terrain model again in boreal forests (Karila et al. 2015).

The potential of airborne X- and P-band InSAR for canopy height estimation was evaluated in tropical forests (Rombach and Moreira 2003; Gama, Dos Santos, and Mura 2010; Neeff et al. 2005). For instance, Neeff et al. (2005) demonstrated the potential of such an airborne InSAR for canopy height ($R^2 = 0.83$, root mean square error [RMSE] = 4.1 m) and biomass estimation ($R^2 = 0.89$, cross-validated RMSE = 46.1 t ha⁻¹) in the tropical forest of the Amazon basin. Space borne TanDEM-X was used together with lidar, optical imagery and L-band data from ALOS PALSAR to estimate biomass and forest area in the Miombo woodlands of Tanzania, whereas TanDEM-X was considered less important than high resolution optical images from RapidEye (Naesset et al. 2016). It is worth noting that the Miombo woodlands of Tanzania have significantly lower biomass compared to dense tropical forest (Solberg et al. 2015a). Treuhaft et al. (2015) estimated aboveground biomass with errors about 29–35% combining means of the interferometric height, lidar terrain height and interferometric coherence from TanDEM-X and suggested that those results require further research.

In addition, Solberg et al. (2013, 2014, 2015a) achieved high accuracies in deforestation and biomass change mapping by using the combination of different X-band height models from SRTM and TanDEM-X. Nevertheless, this biomass change approach requires knowledge about the relationship of InSAR height and biomass in order to convert the X-band InSAR height changes to biomass (Solberg et al. 2015a, 2014). However, this knowledge is lacking in tropical forests since most of the studies using space borne data such as the TanDEM-X heights were based in boreal forests (Solberg et al. 2015a; Rahlf et al. 2014; Solberg et al. 2014; Sadeghi, Leblon, and Simard 2016; Karila et al. 2015).

All the aforementioned studies have the main challenge of the availability of a DTM representing the bare earth height for CHM creation in common. Most of them, especially the TanDEM-X studies, used lidar to retrieve the terrain height (e.g. Sexton et al. 2009; Solberg et al. 2010; Solberg et al. 2013; Rahlf et al. 2014; Treuhaft et al. 2015; Sadeghi, Leblon, and Simard 2016; Karila et al. 2015), but also the interferometric SAR exploitation of long wavelengths (Balzter, Rowland, and Saich 2007; Sexton et al. 2009; Gama, Dos Santos, and Mura 2010; Hansen et al. 2015) or other data sources such as topographic maps (Weydahl et al. 2007; Kelldorfer et al. 2004; Hyde et al. 2006) could be utilized.

On the basis of the statements above, the objectives of this research are two folds. TanDEM-X surface models were assessed and considered high accurate surpassing mission requirements in moderate relief, whereas assessments in tropical forest conditions on local scale are lacking (Balzter, Baade, and Rogers 2016; Wessel et al. 2014). A DTM is retrieved from the TanDEM-X DEM and no validation of TanDEM-X terrain models is known to the authors. Therefore, the first main objective of this study is the verification of digital surface and DTM from TanDEM-X in a tropical forest. Furthermore, the potential of the DTM for canopy height and biomass estimation is assessed in order to overcome the limitations of using an external terrain model dataset.

Second, previous results suggest that the potential of space borne X-band interferometric height for CHM and further biomass estimation in tropical forests require more research (Naesset et al. 2016; Treuhaft et al. 2015). However, the relationship of X-band InSAR height and biomass is of high importance in order to estimate the biomass if a terrain model exists or in biomass change assessments comparing two X-band InSAR heights (Solberg et al. 2014, 2015a). Therefore, the second main objective is the analysis of TanDEM-X height in combination with a high accurate terrain model for canopy height and biomass estimation of tropical forests in order to confirm promising results from boreal forests (Solberg et al. 2013; Rahlf et al. 2014; Sadeghi, Leblon, and Simard 2016; Karila et al. 2015). Potentially, the TanDEM-X surface height could be used as homogeneous and consistent data source in combination with any terrain model in order to estimate canopy height and biomass. Even outdated or future acquired terrain models could be used assuming that the terrain is constant over time, which is in most cases a realistic assumption. In addition, the found X-band InSAR height and biomass relationship of tropical forests within this study could be further utilized in biomass change assessments, e.g. suggested by Solberg et al. (2015a).

2. Study area

The study area is located in Central Kalimantan and is about 60 km west of the provincial capital Palangkaraya. In general, the climate is humid tropic divided into an averaged dry season from June to September and a wet season from October to May (Jauhiainen et al. 2005). The study area exhibits a flat terrain and is covered by tropical peat swamp forest, which is limited through the Kapuas River in the west (Figure 1).

The peat swamp forests in the investigation area are highly endangered despite their importance as carbon storage. The study area was part of the Mega Rice Project (MRP), which was abandoned in 1999 (Muhamad and Rieley 2002; Wösten et al. 2008). The main objective of the MRP was to transform about 1 million hectares of tropical peat lands in rice cultivation. Therefore, the study area is heavily affected by the construction of canals and related deforestation, which is visible in the southern part of the DEM (Figure 1). The lidar and field data were mainly acquired in forested areas belonging to the Mawas conservation area, and thus are undisturbed since the end of the 1990s.

Tropical peat swamp forests differ significantly from tropical dryland forests (Lawson et al. 2015). Peat lands develop usually in low drainage areas with a high water table almost throughout the whole year resulting in a deficit of nutrients and accumulation of organic material (Phillips 1998; Page et al. 1999; Hooijer et al. 2010; Lawson et al. 2015).

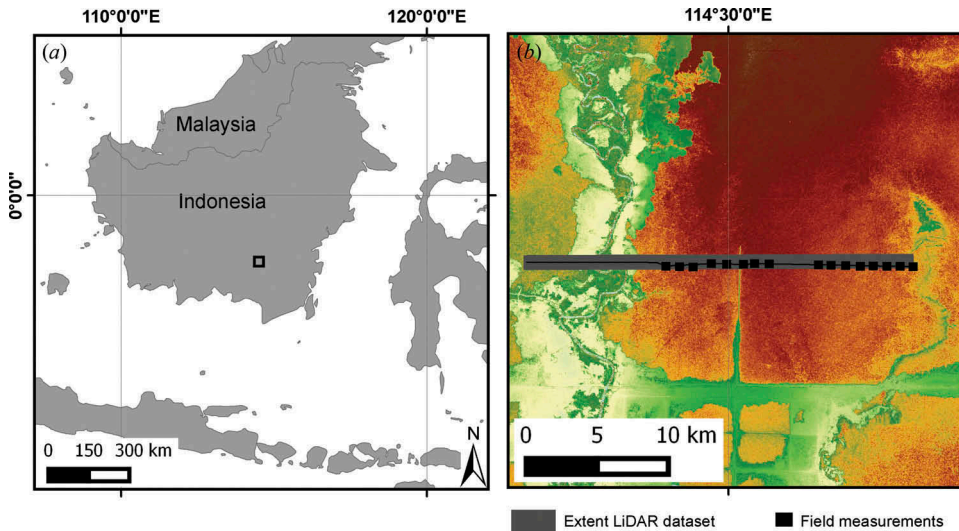


Figure 1. Location of study area in Central Kalimantan, Indonesia (a), and iDEM of study area with location of field plots, lidar transect (grey) and profile from Figures 2 and 6 (black line; b).

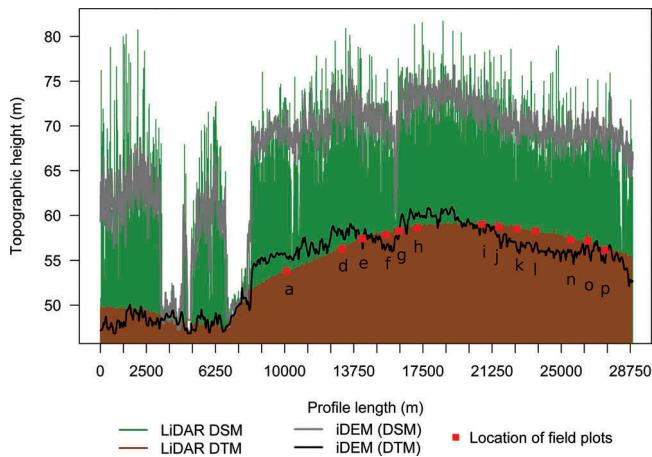


Figure 2. Profile of lidar as well as iDEM DSM and DTM over peat dome (from west to east) with location of field transects.

The study area has a convex topography, which results in a dome shaped terrain typical for many peat lands (Figure 2; Phillips 1998).

The largest peat layer is at the top of the peat dome with decreasing peat thickness towards the edge of the dome (Sorensen 1993; Phillips 1998; Page et al. 1999). The nutrients are elutriated from the top, and thus the nutrient level decreases from the edges towards the top of the peat dome (Phillips 1998; Sorensen 1993; Page et al. 1999). This nutrient distribution results in a typical species composition and forest structure. Forests with high trees up to 35 m and high biomass are located towards the edge of the peat dome close to the river (Figures 2 and 3). The height and biomass of the trees

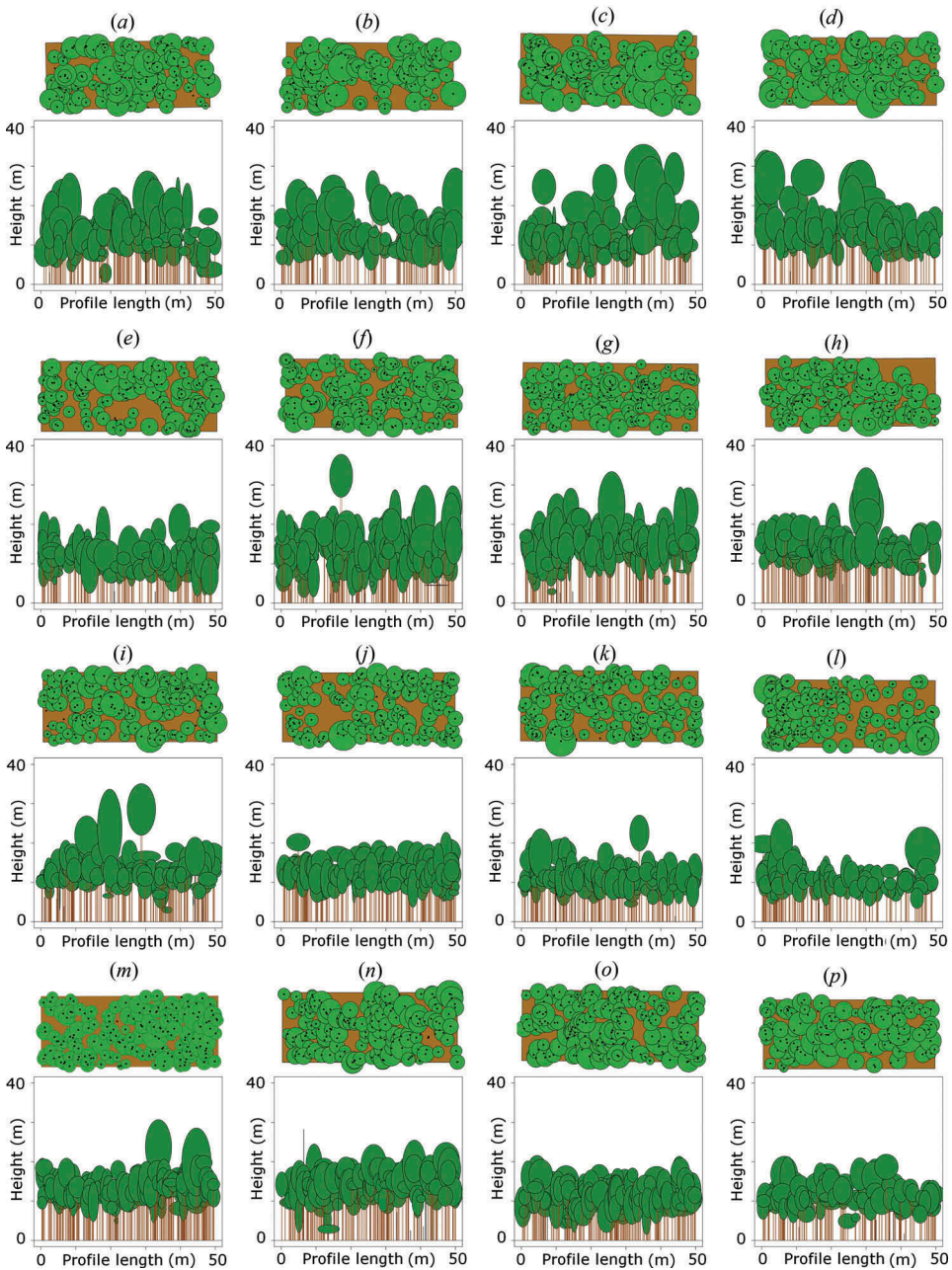


Figure 3. Physiognomic – structural profiles of the 16 field plots allocated along the transect.

decreases towards the top of the peat dome, whereas the tree density increases (Figures 2 and 3; Sorensen 1993; Page et al. 1999). Physiognomic and structural profiles were created from field measurements (see Section 3.3) showing the transition from tall trees to smaller and thin trees, whereas increase in number of trees within the field transect. Field plots (a) to (d) are heterogeneous with dominating large trees resulting in high biomass, whereas (j) to (p) exhibit small trees with a homogeneous height (Figure 3).

3. Data description

3.1 Interferometric height models

TanDEM-X intermediate digital elevation model (iDEM) was used in this study, which was produced and released by German Aerospace Center (DLR) in 2014. This DEM was created by using a close formation of the TerraSAR-X and TanDEM-X X-band SAR satellites with a wavelength of about 3.1 cm. Interferometric data of the entire land mass was acquired several times between 2010 and 2014. The data for the creation of the global DEM were acquired in the horizontal polarization (HH) using the bistatic acquisition in StripMap mode (i.e. one satellite transmits the SAR signal and both receive the signal simultaneously from different orbit positions resulting in negligible temporal decorrelation effects) (Krieger et al. 2007).

The iDEM was created using only one baseline configuration out of several interferometric acquisitions of the mission's first year. The final product of the TanDEM-X WorldDEM™ will be created out of multiple acquisitions and baseline configurations in order to fulfil the specified vertical accuracy (Krieger et al. 2007; Airbus Defence and Space 2014). Thus, the accuracy of this intermediate product (iDEM) may be lower than the WorldDEM™. However, it can be argued that the assessment of its potential for aboveground biomass estimations is already useful with the iDEM. This is due to the similar data source and processing differing only in the multiple-baseline phase unwrapping, affecting mainly mountainous regions (Wessel et al. 2013). In addition, the heights of forests found to be stable over different acquisitions suggesting that the acquisition date and number of acquisitions plays a minor role for canopy height and biomass estimation (Solberg, Lohne, and Karyanto 2015b, 2015c). The iDEM tile used in this study was created with TanDEM-X acquisitions from 21 December 2010 to 15 January 2012 covering a $1^\circ \times 1^\circ$ cell.

Geo-Intelligence of Airbus Defence and Space created in a semi-automated process a DTM representing the bare earth terrain on the basis of the iDEM. This DTM was used in this study and was provided by Geo-Intelligence of Airbus Defence and Space. First, objects were delineated and their height estimated. Second, this estimated height was subtracted from the respective objects. Finally, small objects were removed and the terrain height interpolated. Both interferometric height models had a posting of about 12 m ($0.4' \times 0.4'$; Wessel et al. 2013; Airbus Defence and Space 2014).

3.2 Lidar height models

Full-waveform lidar data were acquired on 5 August 2007 on a sunny and cloud-free day with a Riegl LMS-Q560 instrument (Table 1). The helicopter with the Riegl LMS-Q560 instrument had an altitude of 500 m above ground. The laser range finder system LMS-Q560 acquired up to four returns of the signal from ground, whereas only first and last pulse laser echoes were used. The acquisition date was in the dry season in order to avoid inaccurate derivation of the DTM due to high water levels on the ground. The laser beams were classified with a terrain-adaptive bare earth algorithm into ground and over ground classes. Delaunay triangulation was utilized in order to create a triangular irregular network (TIN). This was the basis for the extraction of square grid pixels with

Table 1. Properties of the airborne lidar system LMS-Q560 (Riegl).

Property	Value
Scan angle (field of view)	$\pm 30^\circ$
Swath width	About 500 m
Scan frequency	66–100 kHz
Vertical laser beam accuracy	≤ 0.1 m
Horizontal laser beam accuracy	≤ 0.5 m (for x- and y-direction)
Laser beam (mrad)	0.5 (footprint up to 30 cm)
Laser wavelength	1.5 μm (near-infrared)
Point density	1.4 points m^{-2}

a linear interpolation for ground and over ground layers representing a terrain model and a surface model (Boehm, Liesenberg, and Limin 2013; Liesenberg et al. 2013). The filtering and classification of DSM and DTM were conducted in an IDL software package used by company Milan (Boehm, Liesenberg, and Limin 2013). The final dataset had a horizontal resolution of 1 m and a vertical resolution of 0.15 m. The lidar dataset covered about 34 km^2 of the iDEM.

3.3 Field data

Field measurements were conducted in 2013 and 2014. A transect along west-east direction in the study area covering the whole peat dome from riverine forest to low pole forest were used to sample field plots systematically every kilometre (Figure 1). Hence, a large range and variability of aboveground tree biomass values within a tropical peat swamp forest were covered despite the difficult accessibility of the area. In total, 16 sample plots with a size of 50 m \times 20 m were measured. The small size of field plots was chosen assuming no drastic change of the forest within the length of the plots in order to sample more field plots in this peat swamp forest. All field plots were located with GPS with a specified accuracy of 3 m. The height and diameter of all trees with a diameter at breast height (dbh) larger than 10 cm within a plot were measured and tree species recorded (Table 2). About 35 species per plot in average were present.

In total, 16 field plots with tree measurements were located within iDEM and 13 within lidar coverage. The field measurements covered a range of aboveground biomass between 250 and 450 t ha^{-1} (see Section 4.2 for aboveground biomass calculation). A vertex clinometer was used for the tree height measurements. The stems of the measured peat swamp forest trees were relatively thin (in average 14.4 cm; Table 2) and most of them were regularly shaped. Irregular cross sections of stems were not handled individually. Parts of the field measurements were re-measured by a second independent team with the same instruments. This resulted in low discrepancies and high correlation between the measurements ($R^2 > 0.9$) suggesting reliable analysis.

Table 2. Field measurements and according mean, minimum, and maximum of all measured trees.

Measurement	Mean	Minimum	Maximum
Tree height (m)	15.6	5.3	37.8
Height of first green branch (m)	9.6	1.5	26.9
DBH (cm)	14.4	10	63.3
Average number of trees ha^{-1}	1329.4	–	–

4. Methods

4.1 Verification of height models

The accuracy of the iDEM and the derived DTM was assessed by comparison with the respective lidar DSM and DTM. For this purpose, the lidar elevation models were aggregated and bilinear resampled to similar pixel-size as the iDEM (12 m). Different CHMs were calculated by subtracting the lidar DTM from lidar DSM (CHM_{lidar}), the lidar DTM from iDEM ($CHM_{\text{iDEM/lidar}}$) as well as the iDEM from iDEM DTM (CHM_{iDEM} ; Table 3; Figure 4).

In order to evaluate the different height models quantitatively, a statistical analysis on pixel level was carried out. The RMSE and linear error of 90% (LE90) were used. The RMSE was calculated with the following formula:

$$RMSE = \sqrt{\frac{1}{N} \sum_{i=1}^N (y_i - \bar{y})^2} \text{ and } RMSE \text{ (in \%)} = \frac{(RMSE)}{\bar{y}} \times 100. \quad (1)$$

The LE 90 is a commonly used criterion to evaluate a DEM in vertical dimensions describing the vertical distance in which 90% of the control points and corresponding model values can be found. The mean error (ME), standard error (SE), and a ratio of both errors (k) were used to calculate the LE90:

Table 3. Overview of available canopy height models.

Canopy height model	Input DSM	Input DTM	Original spatial resolution	
			(m)	Number of used field transects
CHM_{iDEM}	iDEM DSM	iDEM DTM	12	16
$CHM_{\text{iDEM/lidar}}$	iDEM DSM	lidar DTM	12	13
CHM_{lidar}	lidar DSM	lidar DTM	1	13

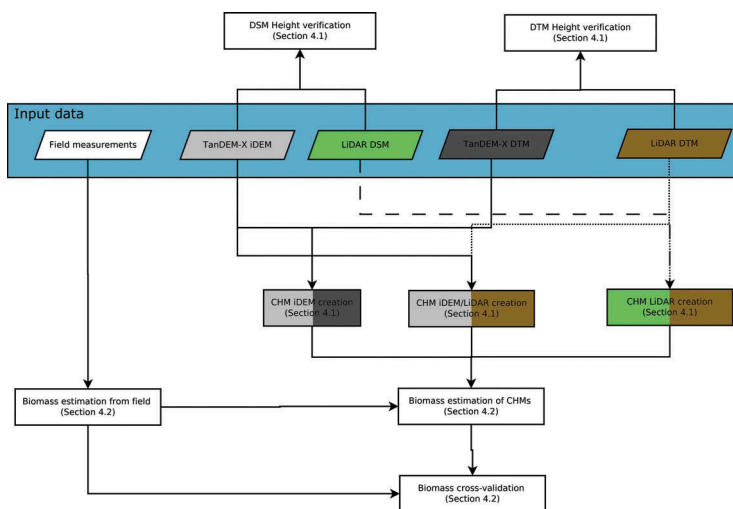


Figure 4. Overview of simplified methodological flowchart.

$$ME = \frac{1}{N} \sum_{i=1}^N y_i - \hat{y}_i, \quad (2)$$

$$SE = \sqrt{\frac{1}{N-1} \sum_{i=1}^N (y_i - \hat{y}_i)^2}, \quad (3)$$

$$k = 1.6435 - \left(0.999556 \frac{(ME)}{(SE)}\right) + \left(0.923237 \frac{(ME)}{(SE)}\right) - \left(0.282533 \times \frac{(ME)}{(SE)}\right), \quad (4)$$

$$LE90 = (ME) + (k(SE)), \quad (5)$$

The relative volume error (VE_{rel}) was calculated in order to estimate the systematic over – or underestimation of the model:

$$VE_{rel} = 100 \times \frac{\sum_{i=1}^n (y_i - \hat{y}_i)}{\sum_{i=1}^n (y_i)}, \quad (6)$$

Positive values indicate a systematic underestimation of the model *versus* the reference whereas negative values indicate a systematic overestimation of the model against the reference. In addition, the coefficient of determination (R^2) was calculated as follows:

$$R^2 = 1 - \frac{\sum_{i=1}^n (y_i - \hat{y}_i)^2}{\sum_{i=1}^n (y_i - \bar{y})^2}, \quad (7)$$

where y_i is the actual value of i and \hat{y}_i the predicted value of i , and \bar{y} is the mean of actual values. The accuracy of the DSM was assessed over ground cover types with and without vegetation, where no penetration differences between lidar and SAR could be assumed. Areas without vegetation cover were delineated where the lidar CHM was below 2 m. In addition, the CHM_{iDEM} as well $CHM_{iDEM/lidar}$ were verified against CHM_{lidar} in order to assess the error propagation into CHMs for biomass estimation.

4.2 Biomass estimation and verification

The aboveground tree biomass density in tonnes per hectare for each field plot was calculated using different allometric equations based on stand tables and volume data (Figure 4). Lawson et al. (2015) suggested that standard allometric equations have to be tested in peat forests since they were not developed for peat forests. Nevertheless, the choice was in favour of global or pan-tropical models (Brown and Iverson 1992; Brown and Lugo 1992; Brown, Gillespie, and Lugo 1989; Chave et al. 2005; Hajnsek and Hoekman 2006; Chave et al. 2014), because these are based on a large number of destructive measurements (Brown and Iverson 1992; Brown and Lugo 1992; Brown, Gillespie, and Lugo 1989; Chave et al. 2005; Reyes et al. 1992; Manuri et al. 2014). Regional or local models exhibit a higher risk of biased predictions due to the small sample size (Chave et al. 2005; Manuri et al. 2014). The aboveground tree biomass density used as field reference for each field plot was calculated, according to following allometric equations (Brown and Lugo 1992; Hajnsek and Hoekman 2006):

$$\text{biomass} = v_{\text{ob}} \times w_{\text{d}} \times b_{\text{ef}} (\text{ha}^{-1}), \quad (8)$$

where v_{ob} is the volume over bark, w_{d} is volume-weighted average wood density, which was determined as 0.57 t m^{-3} representing the arithmetic mean for Asian forests (Reyes et al. 1992). The b_{ef} is the biomass expansion factor in order to include leaves, twigs, and branches. The volume over bark was calculated as the sum of bole volume:

$$\text{bolevolume} = b \times h \times s, \quad (9)$$

where b means basal area, h tree height, and s shape factor of 0.7. The biomass expansion factor for bole volume equal or larger than 190 t ha^{-1} was determined as 1.74. The biomass expansion factor for a bole volume (b_{v}) below 190 t ha^{-1} was calculated (Brown and Lugo 1992):

$$b_{\text{ef}} = \exp(3.213 - 0.506 \ln(b_{\text{v}})). \quad (10)$$

Mean values of the different CHMs were extracted for each field plot. Each 0.1 ha grid cell contained about 10 pixels with a pixel spacing of 12 m for iDEM models. It can be assumed that this yielded stable results due to the high accuracy in this iDEM sample (see Section 5.1). The aboveground biomass value for each plot was correlated with the corresponding mean value of the CHM from iDEM (CHM_{iDEM} as well as $\text{CHM}_{\text{iDEM/lidar}}$) and $\text{CHM}_{\text{lidar}}$ (Figure 4). A linear model via least squares regression fitting (Seber and Lee 2003) was applied for the different CHMs and aboveground biomass. Not all field plots were located within the lidar dataset. Those field plots were not used for any model based on lidar DTM or DSM resulting in a smaller number of field observation with 13 samples (Table 3).

An explicit validation data set was not available due the difficult accessibility of the area resulting in the low number of field plots. Therefore, a k -fold cross-validation was applied in order to estimate the goodness of the models (Breiman et al. 1984; Kohavi 1995), where k was set to 10. The 10-fold cross-validation was frequently used and recommended for such purposes (Molinaro, Simon, and Pfeiffer 2005; Kohavi 1995; Breiman and Spector 1992; Breiman 1996).

5. Results

5.1 Goodness of the height models

The iDEM DSM achieved an RMSE of 0.74 m and a LE90 of 0.79 m compared to lidar measurements in areas without vegetation cover without any significant over- or underestimation ($\text{VE}_{\text{rel}} = 0.1\%$, Figure 6). The main topologic features were clearly visible in both models (Figure 5). Including areas with vegetation cover, the accuracy decreased to an RMSE of 5.1 m and a LE90 of 7.48 m (Table 4). The observed VE_{rel} of -3% revealed a small systematic overestimation. The investigations confirmed that the value variations were much smaller in the iDEM DSM compared to lidar DSM (Figures 2 and 6).

The iDEM DTM represented the terrain topography in general, with overestimations where taller trees and underestimations where smaller trees were present (Figure 2). The iDEM DTM achieved an RMSE of 1.39 m and LE90 of 1.49 m underneath forest cover (Figure 6). The iDEM DTM showed no systematic over- or underestimation with a relative volume error of 0.1%.

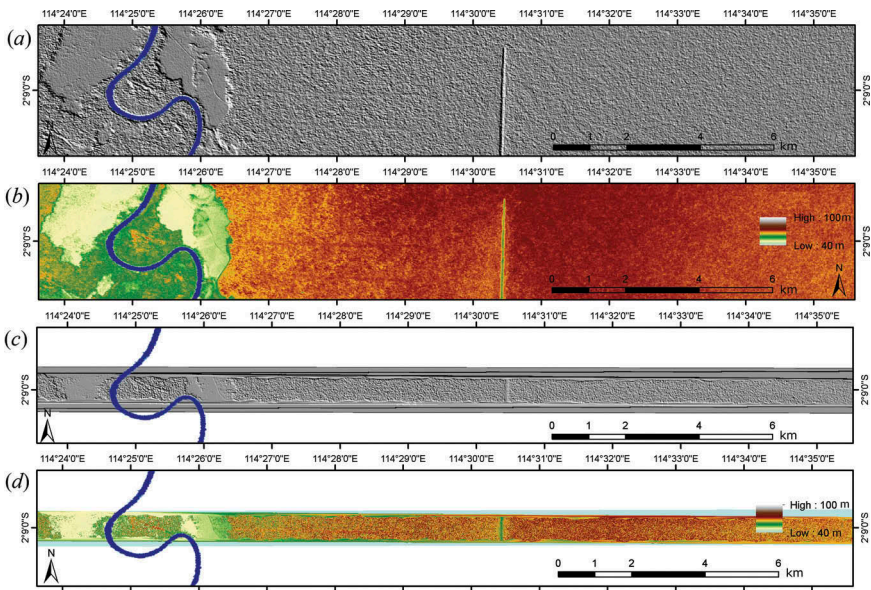


Figure 5. Comparison of iDEM DSM (and corresponding shaded relief; *a* and *b*) and lidar DSM (and corresponding shaded relief, *c* and *d*).

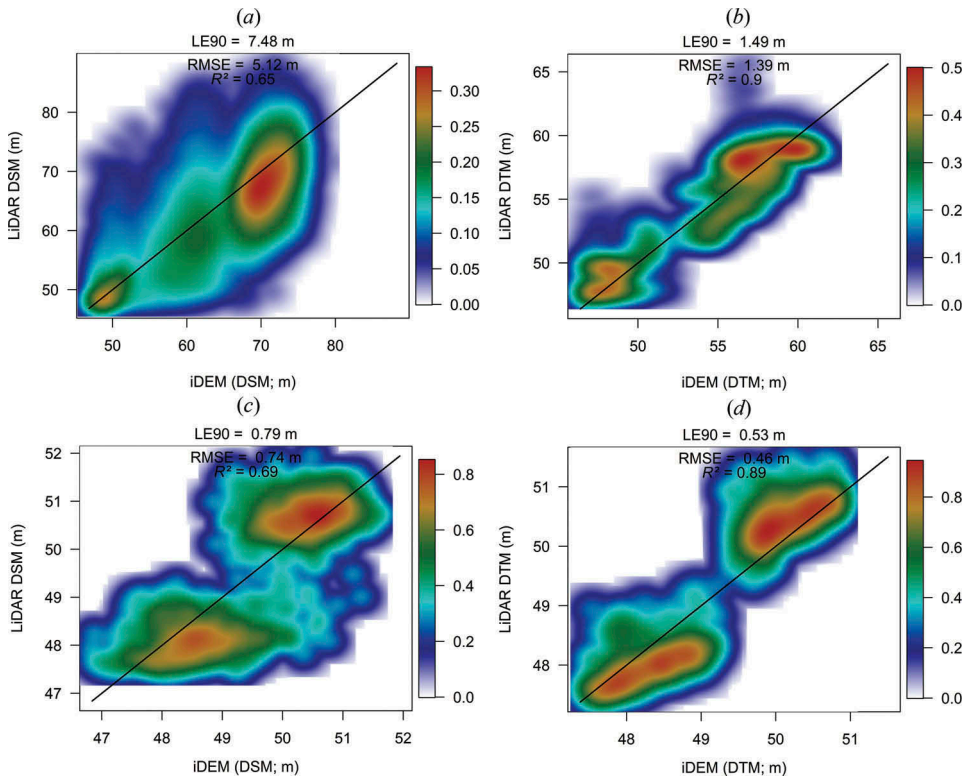


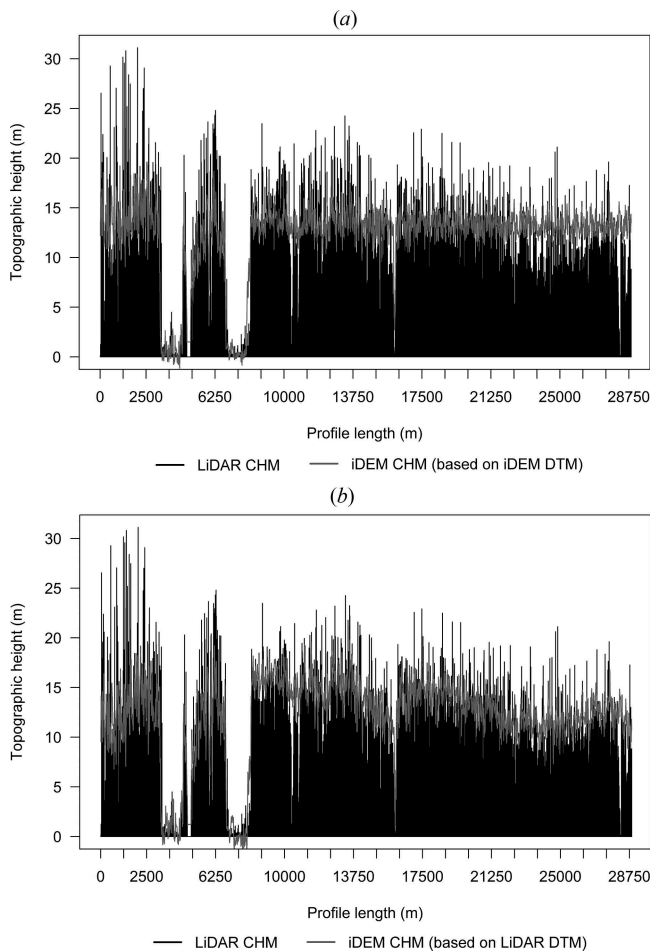
Figure 6. Colour density representation of scatterplots from iDEM DSM (left) and iDEM DTM (right) validation under vegetation cover (top) and without vegetation cover (bottom).

Table 4. Overview of results based on different canopy height models.

Canopy height model	Accuracy of DSM (RMSE [m])	Accuracy of DTM (RMSE [m])	R^2 for aboveground biomass estimation	RMSE in aboveground biomass estimation (t ha^{-1})
CHM _{iDEM}	5.1	1.4	0.18	54.1 (16%)
CHM _{iDEM/lidar}	5.1	–	0.68	24.5 (7.5%)
CHM _{lidar}	–	–	0.75	21.3 (6.5%)

Overall, the iDEM DSM ranged between 47 and 79 m, whereas the corresponding DTM had a value range of 46 and 62 m. The lidar DTM suggested a similar value range of about 47 and 65 m. This confirmed the flatness of the area. The lidar DSM resulted in a similar minimum value of 47 m, but had a higher maximum of about 90 m.

As expected, the errors from both models propagated to the CHM_{iDEM}. Nevertheless, the CHM derived exclusively from iDEM achieved a moderate RMSE of 5.2 m and LE90 of 7.6 m. The lower variations of the DSM and the overestimation of DTM at taller trees and underestimation at smaller trees resulted in a lower spatial variability of the forest canopy height compared to lidar. The CHM_{iDEM} were homogeneous over all forest areas, whereas the CHM_{lidar} indicated trends of lower and higher vegetation. This was clearly visible in the east of the height profile (Figure 7(top)). In contrast, the CHM_{iDEM/lidar} represented differences in

**Figure 7.** Profile of CHM_{lidar} (black) and two different iDEM CHMs (CHM_{iDEM} = a, CHM_{iDEM/lidar} = b).

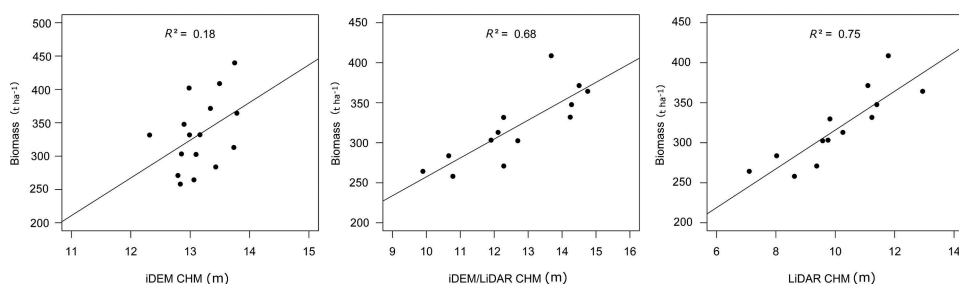


Figure 8. Regression of canopy height models *versus* aboveground biomass.

vegetation height similar to CHM_{lidar} (Figure 7(bottom)). Nevertheless, $CHM_{iDEM/lidar}$ achieved similar accuracies compared to CHM_{iDEM} with an RMSE of 5.1 m and LE90 7.5 m. The CHM based on iDEM had a range from 0 to 25 m, whereas the CHM_{lidar} ranged between 0 and 37 m.

5.2 Biomass estimation

The $CHM_{iDEM/lidar}$ and field measured aboveground biomass showed a coefficient of determination of 0.68 (Figure 8). The CHM_{iDEM} resulted in a substantially lower R^2 of 0.18. The CHM_{iDEM} ranged between 12 m and 14 m for the field plots, whereas the biomass ranged between 258 and 440 t ha⁻¹. In contrast, the $CHM_{iDEM/lidar}$ had a larger range of 9.9 and 14.8 m compared to the CHM_{iDEM} , although the derived biomass range was almost similar (258–410 t ha⁻¹). The CHM_{lidar} ranged between 6.3 and 12.9 m and resulted in a R^2 of 0.75 (Figure 8).

Despite the low coefficient of determination for the CHM_{iDEM} , the 10-fold cross-validation resulted in a moderate average RMSE of 54.1 t ha⁻¹ representing 16.3% of the mean biomass. The moderate RMSE could be related to the low variation of heights within the CHM_{iDEM} . As expected due to the substantial higher R^2 , the other CHMs resulted in substantially lower average RMSEs of 24.5 t ha⁻¹ (7.5%; $CHM_{iDEM/lidar}$) and 21.3 t ha⁻¹ (6.5%, CHM_{lidar}), respectively (Table 4). The uniform CHM_{iDEM} resulted in weak biomass differences along the transect, whereas the $CHM_{iDEM/lidar}$ and CHM_{lidar} biomass estimation clearly indicated high biomass in the west close to the river and lower biomass in the east and at the top of the peat dome (Figure 9). However, the range of all biomass estimations was similar in forested areas with about 200 and 500 t ha⁻¹.

6. Discussion

6.1 Height accuracy and implications for CHMs

The differences of iDEM and lidar height have multiple reasons. First, the acquisition geometry of an InSAR and lidar system is different. The iDEM was acquired with a space borne SAR interferometer, which acquired the data in side-looking geometry with incidence angles of about 30–50°. This results in a lower probability to detect the ground or smaller trees in openings of the forest canopy compared to a lidar system with scan angles of $\pm 30^\circ$. Second, the resolution of both systems is different. The lidar signals were

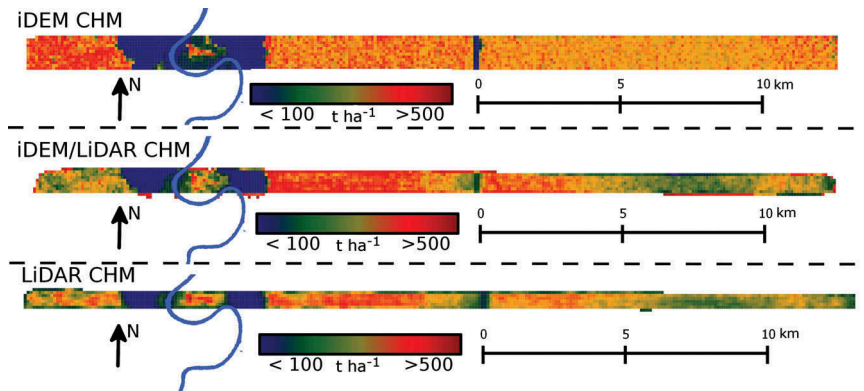


Figure 9. Comparison of aboveground biomass estimation from CHM_{iDEM} (top), $CHM_{iDEM/lidar}$ (centre), and CHM_{lidar} (bottom).

classified, filtered, and sampled to a square grid pixel size of 1 m. The iDEM was derived from TanDEM-X StripMap data with a resolution of about 3 m and was posted to 12 m (Wessel et al. 2013). This could explain the local overestimation of iDEM compared to lidar despite the penetration depth of X-band InSAR. Sadeghi, Leblon, and Simard (2016) observed a similar local overestimation of SAR compared to lidar in boreal forests, which was similarly to our study related to the resolution difference and side looking effect. Third, short wavelength of X-band interacts mainly with constituents of the upper canopy resulting in a low penetration depth, which is a result of height and density of the forest (Solberg et al. 2010; Dobson et al. 1995; Treuhaft and Siqueira 2004; Askne et al. 2013). Differences in signal sampling resolution and averaging for noise reduction in combination with side-looking geometry and low penetration depth explain the lower amplitude and variation of the iDEM compared to lidar.

Wallington and Woodhouse (2004) found low accuracies for DTM generated from X-band InSAR interpolation, resulting in low accuracies in the CHM (RMSE = 23.5 m). In contrast, the iDEM DTM achieved high accuracies with and without vegetation cover. Nevertheless, the reconstruction and quality of the terrain model largely depends on ground visibility and complexity of the terrain. Generally, the actual terrain height values are lowest where the highest vegetation existed, whereas highest terrain values are present where the lowest vegetation occurred. Therefore, the DTM follows the canopy surface, thus resulting in an almost constant CHM. The inaccuracies of iDEM DSM and iDEM DTM propagated into the canopy height estimation. Nevertheless, the RMSE of the CHM_{iDEM} is similar to other CHM estimations with InSAR (Neeff et al. 2005; Balzter, Rowland, and Saich 2007; Rombach and Moreira 2003; Hyde et al. 2006). As expected, CHM based on combination of InSAR surface height and lidar terrain height achieved higher accuracies.

Accurate DTMs can be created out of multiple sources like lidar or long wavelength SAR. It could be expected that the existence of DTMs will increase in the future. For instance, the ESA's BIOMASS mission will exploit P-band InSAR in order to create a terrain model (ESA 2012), which could be used for canopy height estimations with high accuracy (Hansen et al. 2015; Neeff et al. 2005). Assuming that the terrain will not change drastically over time, TanDEM-X height models can be used with any past or

future terrain model to create CHM representing the status from 2010 to 2014. Previous studies showed the potential of TanDEM-X in combination with lidar in boreal and Miombo forests (Sadeghi, Leblon, and Simard 2016; Solberg et al. 2013; Rahlf et al. 2014; Naeset et al. 2016), which was confirmed for tropical forests in this study.

6.2 Biomass estimation with CHMs

The biomass estimations resulted in relative RMSE of 16% for TanDEM-X-based CHM_{iDEM} compared to 6.5% for lidar-based CHM_{lidar} and 7.5% for the combination of both sources ($CHM_{iDEM/lidar}$). Since the $CHM_{iDEM/lidar}$ and CHM_{lidar} resulted in a similar RMSE, it could be argued that the iDEM DSM is suitable to estimate aboveground biomass with high accuracy in cases where an accurate terrain model exists. Again, any terrain model could be used in combination with globally consistent TanDEM-X dataset to create a CHM. The iDEM DTM can be used to produce a CHM in case of unavailability of highly accurate terrain model. This has large impact on the accuracy of the estimation and provides only an indication of biomass.

It was previously found that lidar compared to InSAR resulted in significantly lower RMSE in biomass estimations in boreal forests or temperate forests (Rahlf et al. 2014; Naeset et al. 2011, 2016; Hyde et al. 2006). This was not confirmed by this study in tropical forests showing similar RMSE values for $CHM_{iDEM/lidar}$ and CHM_{lidar} . The height and density of the forest influence the resulting surface height of X-band InSAR estimate, whereas both parameters explain the biomass variation to a large extent (Askne et al. 2013; Treuhaft and Siqueira 2004; Solberg et al. 2010). Therefore, it could be argued that the InSAR surface height estimation can achieve comparable accuracies to lidar. The iDEM performed similar or better to previously investigated biomass estimations in tropical forests based on airborne InSAR CHMs (Neeff et al. 2005; Gama, Dos Santos, and Mura 2010; Treuhaft et al. 2009). For instance, Treuhaft et al. (2009) estimated the aboveground biomass of tropical forests in Costa Rica resulting in an accuracy of 30%. Neeff et al. (2005) reported a cross-validated RMSE of 46.1 t ha^{-1} on basis of an InSAR CHM and P-band backscatter, whereas Gama, Dos Santos, and Mura (2010) reported an RMSE of 16 t ha^{-1} (20% of mean biomass). Treuhaft et al. (2015) also demonstrated the high potential of TanDEM-X heights in combination with interferometric coherence in tropical forests, which was confirmed in our study by using the height only. In addition, the found relationship of TanDEM-X InSAR heights in tropical forests is usable in biomass change estimation based on X-band InSAR height differences (Solberg et al. 2014, 2015a).

Biomass estimations in tropical peat swamp forest based on combination of field measurements and lidar data resulted in 20–40% errors (Boehm, Liesenberg, and Limin 2013; Kronseder et al. 2012; Englhart, Jubanski, and Siegert 2013; Ballhorn, Jubanski, and Siegert 2011). SAR data was also frequently used to estimate biomass of tropical peat swamp forests (Englhart, Keuck, and Siegert 2011; Morel et al. 2011; Schlund et al. 2015). SAR backscatter based methods suffer mostly from saturation effects, whereas saturation at 88 t ha^{-1} for L-band and 80 t ha^{-1} for X-band were suggested (Morel et al. 2011; Englhart, Keuck, and Siegert 2011). The biomass of the investigated area is exceeding this saturation limit for majority of the forest area. Exploiting the phase of the SAR signal using the coherence increased the saturation level and accuracy (Schlund et al. 2015). The measurement of the canopy height for estimating biomass could overcome the current saturation limitations for short wavelength SAR systems.

6.3 Up-scaling of biomass from field measurements

Only a few field measurements are necessary to transform lidar metrics to biomass (Asner et al. 2009). A prerequisite of this assumption is the distribution of the field measurements over the entire range of biomass. The field measurements were sampled systematically on a transect over the peat dome. Therefore, it could be assumed that the whole range of biomass was covered with 250–450 t ha⁻¹ despite the difficult terrain accessibility. Nevertheless, more ground reference could potentially improve the estimation of biomass and its uncertainty analysis using an explicit validation data set. In general, studies in tropical peat swamp forests need more field measured data to increase confidentiality. However, as explained before this is hardly achievable due to their remoteness and frequently high water tables (Lawson et al. 2015; Phillips 1998).

Additional errors may result from different acquisition dates of field measurements and remote sensing data (i.e. the lidar dataset 2007 vs 2014). However, the study area is part of a conservation area where the forests are relatively undisturbed since the abandonment of the MRP in 1999 (Aldhous 2004). Moreover, investigations showed that the biomass increases only marginally in undisturbed peat swamp forests of Central Kalimantan as well as in the study area (Boehm et al. 2012; Boehm, Liesenberg, and Limin 2013; Englhart, Jubanski, and Siegert 2013; Sweda et al. 2012). Therefore, it can be concluded that inconsistencies between the different acquisition dates are minimal and may not affect the results substantially.

GPS localization is also an error source to be considered. However, assuming no drastic change of the forest structure within the field plots and sampling the biomass to 0.1 ha or coarser minimizes the error of GPS localization inaccuracies. Another source of error to be considered is the transformation of field measurements to biomass with allometric equations. Lawson et al. (2015) suggested pan-tropical equations could not be suitable to apply on tropical peat land. This requires confirmation, but it could be argued that the advantage of using a local model with low number of samples will not compensate the potential bias compared to pan-tropical equations with large number of samples (Chave et al. 2005; Manuri et al. 2014; Lawson et al. 2015). Therefore, several pan-tropical allometric equations were tested in order to select the most appropriate for biomass estimation in the peat swamp forest investigated. The choice was guided by the goal to attain similar values as other studies conducted in peat swamp forests. In addition, statistical values of the field measurements were compared to other studies in order to achieve comparable results. The statistical distributions of dbh and tree height measured in peat swamp forests were similar to other studies (Page et al. 1999; Nishimua et al. 2007; Boehm, Liesenberg, and Limin 2013).

The field measurements resulted in an average biomass of 330 t ha⁻¹, whereas the range was 250–450 t ha⁻¹. The derived biomass is in the order of other studies in peat swamp forests of southeast Asia (Table 5). Therefore, it can be concluded that the biomass values used in this study are representative and can be used for the purpose of this study. The differences in those estimates could of course be related to the different geographical locations and the associated conditions as well as different allometric equations used for biomass calculation.

Table 5. Comparison of aboveground biomass values from different studies in southeast Asia.

Aboveground biomass (t ha ⁻¹)	Area	Source
0–370	Sebangau National Park (Central Kalimantan)	Boehm, Liesenberg, and Limin (2013); Enghart, Keuck, and Siegert (2011); Kronseder et al. (2012)
228	Sebangau National Park (Central Kalimantan)	Kronseder et al. (2012)
248–311	Sebangau National Park (Central Kalimantan)	Waldes and Page (2002)
264–397	Southeast Asia	Verwer and van der Meer (2010)
287–491	Thailand	Kaneko (1992)
359.6 ± 76.4	Java, Borneo and Peninsular Malaysia	Koh et al. (2011); Koh et al. (2012); Murdiyarmo, Hergoualc'h, and Verchot (2010)

7. Conclusions

Although based on iDEM precursor data, the results of this study demonstrate that the final TanDEM-X elevation model WorldDEMTM has high potential in combination with high accurate terrain information for estimation of CHMs and aboveground biomass of tropical forests. The found relationship can be also utilized in biomass change estimations based on canopy height comparison. The WorldDEMTM will be globally consistent available resulting in potential cost-efficient and consistent surface estimations usable for canopy height estimation with any terrain information.

The iDEM (especially in combination with an accurate DTM) resulted in a CHM, showing high correlation with biomass ($R^2 = 0.68$). However, an accurate DTM is not always available. The iDEM or WorldDEMTM can be used for reconstructing a terrain model, achieving a high accuracy in relatively flat terrain without vegetation cover. The combination of iDEM DSM and iDEM DTM resulted in a reliable estimation of a CHM, with an RMSE of 5 m compared to lidar reference. However, the terrain model was not able to represent the terrain underneath vegetation cover. This resulted in a uniform CHM yielding poor correlation ($R^2 = 0.18$) and moderate cross-validated RMSE for aboveground biomass estimation of 54 t ha⁻¹ (16%). Nevertheless, it could be argued that this solution can be used where no other biomass information is available resulting in a coarse indication of biomass.

Acknowledgments

The study was funded by Federal Ministry of Economic Affairs and Energy (FKZ 50EE1355), the German Academic Exchange Service and Airbus Defence and Space. The TanDEM-X iDEM were provided by the German Aerospace Center (DLR). BOS is acknowledged for the support in the Mawas field campaigns. We thank the anonymous reviewers for their constructive reviews that substantially improved the manuscript.

Disclosure statement

No potential conflict of interest was reported by the authors.

Funding

This work was supported by Federal Ministry of Economic Affairs and Energy [FKZ 50EE1355], the German Academic Exchange Service and Airbus Defence and Space.

References

- Abdalati, W., H. J. Zwally, R. Bindenschadler, B. Csatho, S. L. Farrell, H. A. Fricker, D. Harding, et al. 2010. "The ICESat-2 Laser Altimetry Mission." *Proceedings of the IEEE* 98 (5): 735–751. doi:10.1109/JPROC.2009.2034765.
- Airbus Defence and Space. 2014. *WorldDEMTM. Technical Product Specification. Version 1.0.*
- Aldhous, P. 2004. "Land Remediation: Borneo Is Burning." *Nature* 432: 144–146. doi:10.1038/432144a.
- Askne, J. I. H., J. E. S. Fransson, M. Santoro, M. J. Soja, and L. M. H. Ulander. 2013. "Model-Based Biomass Estimation of a Hemi-Boreal Forest from Multitemporal TanDEM-X Acquisitions." *Remote Sensing* 5: 5574–5597. doi:10.3390/rs5115574.
- Asner, G. P., R. F. Hughes, T. A. Varga, D. E. Knapp, and T. Kennedy-Bowdoin. 2009. "Environmental and Biotic Controls over Aboveground Biomass Throughout a Tropical Rain Forest." *Ecosystems* 12: 261–278. doi:10.1007/s10021-008-9221-5.
- Baccini, A., N. Laporte, S. J. Goetz, M. Sun, and H. Dong. 2008. "A First Map of Tropical Africa's Above-Ground Biomass Derived from Satellite Imagery." *Environmental Research Letters* 4 (3): 1–9. doi:10.1088/1748-9326/3/4/045011.
- Ballhorn, U., J. Jubanski, and F. Siegert. 2011. "Icesat/GLAS Data as a Measurement Tool for Peatland Topography and Peat Swamp Forest Biomass in Kalimantan, Indonesia." *Remote Sensing* 3: 1957–1982. doi:10.3390/rs3091957.
- Balzter, H., J. Baade, and K. Rogers. 2016. "Validation of the TanDEM-X Intermediate Digital Elevation Model With Airborne LiDAR and Differential GNSS in Kruger National Park." *IEEE Geoscience and Remote Sensing Letters* 13 (2): 277–281. doi:10.1109/LGRS.2015.2509500.
- Balzter, H., C. S. Rowland, and P. Saich. 2007. "Forest Canopy Height and Carbon Estimation at Monks Wood National Nature Reserve, UK, Using Dual-Wavelength SAR Interferometry." *Remote Sensing of Environment* 108: 224–239. doi:10.1016/j.rse.2006.11.014.
- Boehm, H.-D. V., V. Liesenberg, and S. H. Limin. 2013. "Multi-Temporal Airborne LiDAR-Survey and Field Measurements of Tropical Peat Swamp Forest to Monitor Changes." *IEEE Journal of Selected Topics in Applied Earth Observations and Remote Sensing* 6 (3): 1524–1530. doi:10.1109/JSTARS.2013.2258895.
- Boehm, H.-D. V., V. Liesenberg, T. Sweda, H. Tsuzuki, and S. H. Limin. 2012. "Multi-temporal Airborne LiDAR-Surveys in 2007 and 2011 over Tropical Peat Swamp Forest Environments in Central Kalimantan, Indonesia." In Proceedings of the 14th International Peat Congress.
- Breiman, L. 1996. "Stacked Regressions." *Machine Learning* 24 (1): 49–64. doi:10.1007/BF00117832.
- Breiman, L., J. Friedman, C. J. Stone, and R. A. Olshen. 1984. *Classification and Regression Trees*. Wadsworth: CRC press.
- Breiman, L., and P. Spector. 1992. "Submodel Selection and Evaluation in Regression. the X-Random Case." *International Statistical Review* 60: 291–319. doi:10.2307/1403680.
- Brown, S., A. J. R. Gillespie, and A. E. Lugo. 1989. "Biomass Estimation Methods for Tropical Forests with Applications to Forest Inventory Data." *Forest Science* 35: 881–902.
- Brown, S., and L. R. Iverson. 1992. "Biomass Estimates for Tropical Forests." *World Resource Review* 4: 366–384.
- Brown, S., and A. E. Lugo. 1992. "Aboveground Biomass Estimates for Tropical Moist Forests of the Brazilian Amazon." *Interciencia* 17: 8–18.
- Chave, J., C. Andalo, S. Brown, M. A. Cairns, J. Q. Chambers, D. Eamus, H. Fölster, et al. 2005. "Tree Allometry and Improved Estimation of Carbon Stocks and Balance in Tropical Forests." *Oecologia* 145 (1): 87–99. doi:10.1007/s00442-005-0100-x.
- Chave, J., M. Réjou-Méchain, A. Búrquez, E. Chidumayo, M. S. Colgan, W. B. C. Delitti, A. Duque, et al. 2014. "Improved Allometric Models to Estimate the Aboveground Biomass of Tropical Trees." *Global Change Biology* 20 (10): 3177–3190. doi:10.1111/gcb.12629.
- Dandois, J. P., and E. C. Ellis. 2013. "High Spatial Resolution Three-Dimensional Mapping of Vegetation Spectral Dynamics Using Computer Vision." *Remote Sensing of Environment* 136: 259–276. doi:10.1016/j.rse.2013.04.005.

- Dobson, M. C., F. T. Ulaby, L. E. Pierce, T. L. Sharik, K. M. Bergen, J. Kellndorfer, J. R. Kendra, et al. 1995. "Estimation of Forest Biophysical Characteristics in Northern Michigan with SIR-C/X-SAR." *IEEE Transactions on Geoscience and Remote Sensing* 33: 877–895. doi:10.1109/36.406674.
- Drake, J. B., R. O. Dubayah, D. B. Clark, R. G. Knox, J. B. Blair, M. A. Hofton, R. L. Chazdon, J. F. Weishampel, and S. D. Prince. 2002. "Estimation of Tropical Forest Structural Characteristics Using Large-Footprint Lidar." *Remote Sensing of Environment* 79: 305–319. doi:10.1016/S0034-4257(01)00281-4.
- Englhart, S., J. Jubanski, and F. Siegert. 2013. "Quantifying Dynamics in Tropical Peat Swamp Forest Biomass with Multi-Temporal LiDAR Datasets." *Remote Sensing* 5: 2368–2388. doi:10.3390/rs5052368.
- Englhart, S., V. Keuck, and F. Siegert. 2011. "Aboveground Biomass Retrieval in Tropical Forests — The Potential of Combined X- and L-Band SAR Data Use." *Remote Sensing of Environment* 115: 1260–1271. doi:10.1016/j.rse.2011.01.008.
- ESA. 2012. *Report for Mission Selection: Biomass*. ESA SP-1324/1. Noordwijk: European Space Agency.
- Gama, F. F., J. R. Dos Santos, and J. C. Mura. 2010. "Eucalyptus Biomass and Volume Estimation Using Interferometric and Polarimetric SAR Data." *Remote Sensing* 2: 939–956. doi:10.3390/rs2040939.
- Gibbs, H. K., S. Brown, J. O. Niles, and J. A. Foley. 2007. "Monitoring and Estimating Tropical Forest Carbon Stocks: Making REDD a Reality." *Environmental Research Letters* 2: 045023. doi:10.1088/1748-9326/2/4/045023.
- Hajnssek, I., and D. H. Hoekman. 2006. "INDREX II – Indonesian Radar Experiment Campaign over Tropical Forest in L- and P-band. Version 1." Final Report.
- Hansen, E. H., T. Gobakken, S. Solberg, A. Kangas, L. Ene, E. Mauya, and E. Naesset. 2015. "Relative Efficiency of ALS and InSAR for Biomass Estimation in a Tanzanian Rainforest." *Remote Sensing* 7: 9865–9885. doi:10.3390/rs70809865.
- Hooijer, A., S. E. Page, J. G. Canadell, M. Silvius, J. Kwadijk, H. Wösten, and J. Jauhiainen. 2010. "Current and Future CO₂ Emissions from Drained Peatlands in Southeast Asia." *Biogeosciences* 7: 1505–1514. doi:10.5194/bg-7-1505-2010.
- Hyde, P., R. Dubayah, W. Walker, J. B. Blair, M. Hofton, and C. Hunsaker. 2006. "Mapping Forest Structure for Wildlife Habitat Analysis Using Multi-Sensor (Lidar, SAR/Insar, ETM+, Quickbird) Synergy." *Remote Sensing of Environment* 102: 63–73. doi:10.1016/j.rse.2006.01.021.
- Jauhiainen, J., H. Takahashi, J. E. P. Heikkinen, P. J. Martikainen, and H. Vasander. 2005. "Carbon Fluxes from a Tropical Peat Swamp Forest Floor." *Global Change Biology* 11: 1788–1797. doi:10.1111/j.1365-2486.2005.001031.x.
- Kaneko, N. 1992. "Comparison of Forest Structure of Tropical Peat Swamp Forests in Southern Thailand and Malaysia." In *Coastal Lowland Ecosystems in Southern Thailand and Malaysia*, edited by K. Kyuma, P. Vijarnsorn, and A. Zakaria, 152–163.
- Karila, K., M. Vastaranta, M. Karjalainen, and S. Kaasalainen. 2015. "Tandem-X Interferometry in the Prediction of Forest Inventory Attributes in Managed Boreal Forests." *Remote Sensing of Environment* 159: 259–268. doi:10.1016/j.rse.2014.12.012.
- Kellndorfer, J., W. Walker, L. Pierce, C. Dobson, J. A. Fites, C. Hunsaker, J. Vona, and M. Clutter. 2004. "Vegetation height estimation from Shuttle Radar Topography Mission and National Elevation Datasets." *Remote Sensing of Environment* 93: 339–358. doi:10.1016/j.rse.2004.07.017.
- Koch, B. 2010. "Status and Future of Laser Scanning, Synthetic Aperture Radar and Hyperspectral Remote Sensing Data for Forest Biomass Assessment." *ISPRS Journal of Photogrammetry and Remote Sensing* 65: 581–590. doi:10.1016/j.isprsjprs.2010.09.001.
- Koch, B., U. Heyder, and H. Weinacker. 2006. "Detection of Individual Tree Crowns in Airborne Lidar Data." *Photogrammetric Engineering & Remote Sensing* 72 (4): 357–363. doi:10.14358/PERS.72.4.357.
- Koh, L. P., H. K. Gibbs, P. V. Potapov, and M. C. Hansen. 2012. "Reddcalculator.Com: A Web-Based Decision-Support Tool for Implementing Indonesia's Forest Moratorium." *Methods in Ecology and Evolution* 3: 310–316. doi:10.1111/j.2041-210X.2011.00147.x.

- Koh, L. P., J. Miettinen, S. C. Liew, and J. Ghazoula. 2011. "Remotely Sensed Evidence of Tropical Peatland Conversion to Oil Palm." *Proceedings of the National Academy of Sciences* 108 (12): 5127–5132. doi:10.1073/pnas.1018776108.
- Kohavi, R. 1995. "A Study of Cross-Validation and Bootstrap for Accuracy Estimation and Model Selection." In International Joint Conference on Artificial Intelligence (IJCAI), 1137–1143.
- Köhl, M., A. Lister, C. T. Scott, T. Baldauf, and D. Plugge. 2011. "Implications of Sampling Design and Sample Size for National Carbon Accounting Systems." *Carbon Balance Management* 6: 10–20. doi:10.1186/1750-0680-6-10.
- Krieger, G., A. Moreira, H. Fiedler, I. Hajnsek, M. Werner, M. Younis, and M. Zink. 2007. "TanDEM-X: A Satellite Formation for High-Resolution SAR Interferometry." *IEEE Transactions on Geoscience and Remote Sensing* 45: 3317–3341. doi:10.1109/TGRS.2007.900693.
- Kronstedter, K., U. Ballhorn, H.-D. V. Böhm, and F. Siegert. 2012. "Above Ground Biomass Estimation across Forest Types at Different Degradation Levels in Central Kalimantan Using Lidar Data." *International Journal of Applied Earth Observation and Geoinformation* 18: 37–48. doi:10.1016/j.jag.2012.01.010.
- Lawson, I. T., T. J. Kelly, P. Aplin, A. Boom, G. Dargie, F. C. H. Draper, P. N. Z. B. P. Hassan, et al. 2015. "Improving Estimates of Tropical Peatland Area, Carbon Storage, and Greenhouse Gas Fluxes." *Wetlands Ecology and Management* 23 (3): 327–346. doi:10.1007/s11273-014-9402-2.
- Lefsky, M. A., W. B. Cohen, G. G. Parker, and D. J. Harding. 2002. "Lidar Remote Sensing for Ecosystem Studies." *Bioscience* 52 (1): 19–30. doi:10.1641/0006-3568(2002)052[0019:LRFSFES]2.0.CO;2.
- Liesenberg, V., H.-D. V. Boehm, H. Joosten, and S. Limin. 2013. "Spatial and Temporal Variation of above Ground Biomass in Tropical Dome-Shaped Peatlands Measured by Airborne Lidar." In Proceedings of International Symposium on Wild Fire and Carbon Management in Peat-Forest in Indonesia, 99–117.
- Manuri, S., C. Brack, N. P. Nugroho, K. Hergoualc'h, N. Novita, H. Dotzauer, L. Verchot, C. A. S. Putra, and E. Widyasari. 2014. "Tree Biomass Equations for Tropical Peat Swamp Forest Ecosystems in Indonesia." *Forest Ecology and Management* 334: 241–253. doi:10.1016/j.foreco.2014.08.031.
- Molinaro, A. M., R. Simon, and R. M. Pfeiffer. 2005. "Prediction Error Estimation: A Comparison of Resampling Methods." *Bioinformatics* 21 (15): 3301–3307. doi:10.1093/bioinformatics/bti499.
- Morel, A. C., S. S. Saatchi, Y. Malhi, N. J. Berry, L. Banin, D. Burslem, R. Nilus, and R. C. Ong. 2011. "Estimating Aboveground Biomass in Forest and Oil Palm Plantation in Sabah, Malaysian Borneo Using ALOS PALSAR Data." *Forest Ecology and Management* 262: 1786–1798. doi:10.1016/j.foreco.2011.07.008.
- Muhamad, N. Z., and J. O. Rieley. 2002. "Management of Tropical Peatlands in Indonesia: Mega Reclamation Project in Central Kalimantan." In *Peatlands for People: Natural Resource Functions and Sustainable Management. Proceedings of the International Symposium on Tropical Peatland*, edited by J. O. Rieley, S. E. Page, and B. Setiadi, 155–162.
- Murdiyarso, D., K. Hergoualc'h, and L. V. Verchot. 2010. "Opportunities for Reducing Greenhouse Gas Emissions in Tropical Peatlands." *Proceedings of the National Academy of Sciences* 107 (46): 19655–19660. doi:10.1073/pnas.0911966107.
- Naesset, E., T. Gobakken, S. Solberg, T. G. Gregoire, R. Nelson, G. Ståhl, and D. J. Weydahl. 2011. "Model-Assisted Regional Forest Biomass Estimation Using Lidar and Insar as Auxiliary Data: A Case Study from a Boreal Forest Area." *Remote Sensing of Environment* 115: 3599–3614. doi:10.1016/j.rse.2011.08.021.
- Naesset, E., H. O. Ørka, S. Solberg, O. M. Bollandsås, E. H. Hansen, E. Mauya, E. Zahabu, et al. 2016. "Mapping and Estimating Forest Area and Aboveground Biomass in Miombo Woodlands in Tanzania Using Data from Airborne Laser Scanning, Tandem-X, Rapideye, and Global Forest Maps: A Comparison of Estimated Precision." *Remote Sensing of Environment* 175: 282–300. doi:10.1016/j.rse.2016.01.006.
- Neeff, T., L. V. Dutra, J. R. Santos, C. C. Freitas, and L. S. Araújo. 2005. "Tropical Forest Measurement by Interferometric Height Modeling and P-Band Backscatter." *Forest Science* 51 (6): 585–594.

- Nishimua, T. B., E. Suzuki, T. Kohyama, and S. Tsuyuzaki. 2007. "Mortality and Growth of Trees in Peat-Swamp and Heath Forests in Central Kalimantan after Severe Drought." *Plant Ecology* 188: 165–177. doi:10.1007/s11258-006-9154-z.
- Olander, L. P., H. K. Gibbs, M. Steininger, J. J. Swenson, and B. C. Murray. 2008. "Reference Scenarios for Deforestation and Forest Degradation in Support of REDD: A Review of Data and Methods." *Environmental Research Letters* 3: 025011. doi:10.1088/1748-9326/3/2/025011.
- Page, S. E., J. O. Rieley, and C. J. Banks. 2011. "Global and Regional Importance of the Tropical Peatland Carbon Pool." *Global Change Biology* 17: 798–818. doi:10.1111/j.1365-2486.2010.02279.x.
- Page, S. E., J. O. Rieley, O. W. Shotyk, and D. Weiss. 1999. "Interdependence of Peat and Vegetation in a Tropical Peat Swamp Forest." *Philosophical Transactions of the Royal Society B: Biological Sciences* 354: 1885–1897. doi:10.1098/rstb.1999.0529.
- Page, S. E., F. Siegert, J. O. Rieley, H.-D. V. Boehm, A. Jayak, and S. Limink. 2002. "The Amount of Carbon Released from Peat and Forest Fires in Indonesia during 1997." *Nature* 420: 61–65. doi:10.1038/nature01131.
- Phillips, V. D. 1998. "Peatswamp Ecology and Sustainable Development in Borneo." *Biodiversity and Conservation* 7 (5): 651–671. doi:10.1023/A:1008808519096.
- Pitz, W., and D. Miller. 2010. "The TerraSAR-X Satellite." *IEEE Transactions on Geoscience and Remote Sensing* 48: 615–622. doi:10.1109/TGRS.2009.2037432.
- Rahlf, J., J. Breidenbach, S. Solberg, E. Næsset, and R. Astrup. 2014. "Comparison of Four Types of 3D Data for Timber Volume Estimation." *Remote Sensing of Environment* 155: 325–333. doi:10.1016/j.rse.2014.08.036.
- Reyes, G., S. Brown, J. Chapman, and A. E. Lugo. 1992. "Wood Densities of Tropical Tree Species." USDA Forest Service, General Technical Report SO-88. New Orleans, LA: Southern Forest Experiment Station.
- Rombach, M., and J. Moreira. 2003. "Description and Applications of the Multipolarized Dual Band Orbisar-1 Insar Sensor." In Proceedings of the International Radar Conference 2003 IEEE, 245–250.
- Rosette, J. A. B., P. R. J. North, and J. C. Suárez. 2008. "Vegetation Height Estimates for a Mixed Temperate Forest Using Satellite Laser Altimetry." *International Journal of Remote Sensing* 29 (5): 1475–1493. doi:10.1080/01431160701736380.
- Saatchi, S. S., N. L. Harris, S. Brown, M. Lefsky, E. T. A. Mitchard, W. Salas, B. R. Zutta, et al. 2011. "Benchmark Map of Forest Carbon Stocks in Tropical Regions across Three Continents." *Proceedings of the National Academy of Sciences* 108 (24): 9899–9904. doi:10.1073/pnas.1019576108.
- Sadeghi, B. S.-O., B. Leblon, and M. Simard. 2016. "Canopy Height Model (CHM) Derived From a TanDEM-X InSAR DSM and an Airborne Lidar DTM in Boreal Forest." *IEEE Journal of Selected Topics in Applied Earth Observation and Remote Sensing* 9 (1): 381–397. doi:10.1109/JSTARS.2015.2512230.
- Schlund, M., F. Von Poncet, S. Kuntz, C. Schmillius, and D. H. Hoekman. 2015. "Tandem-X Data for Aboveground Biomass Retrieval in a Tropical Peat Swamp Forest." *Remote Sensing of Environment* 158: 255–266. doi:10.1016/j.rse.2014.11.016.
- Seber, G. A. F., and A. J. Lee. 2003. *Linear Regression Analysis*. 2nd ed. New Jersey: Wiley & Sons.
- Sexton, J. O., T. Bax, P. Siqueira, J. J. Swenson, and S. Hensley. 2009. "A Comparison of Lidar, Radar, and Field Measurements of Canopy Height in Pine and Hardwood Forests of Southeastern North America." *Forest Ecology and Management* 257: 1136–1147. doi:10.1016/j.foreco.2008.11.022.
- Simard, M., N. Pinto, J. B. Fisher, and A. Baccini. 2011. "Mapping Forest Canopy Height Globally with Spaceborne Lidar." *Journal of Geophysical Research* 116: 1–12. doi:10.1029/2011JG001708.
- Solberg, S., R. Astrup, J. Breidenbach, B. Nilsen, and D. J. Weydahl. 2013. "Monitoring Spruce Volume and Biomass with Insar Data from Tandem-X." *Remote Sensing of Environment* 139: 60–67. doi:10.1016/j.rse.2013.07.036.

- Solberg, S., R. Astrup, T. Gobakken, E. Naeset, and D. J. Weydahl. 2010. "Estimating Spruce and Pine Biomass with Interferometric X-Band SAR." *Remote Sensing of Environment* 114: 2353–2360. doi:10.1016/j.rse.2010.05.011.
- Solberg, S., R. Astrup, and D. Weydahl. 2013. "Detection of Forest Clear-Cuts with Shuttle Radar Topography Mission (SRTM) and Tandem-X InSAR Data." *Remote Sensing* 5: 5449–5462. doi:10.3390/rs5115449.
- Solberg, S., B. Gizachew, E. Naeset, T. Gobakken, O. M. Bollandsås, E. W. Mauya, H. Olsson, R. Malimbwi, and E. Zahabu. 2015a. "Monitoring Forest Carbon in A Tanzanian Woodland Using Interferometric SAR: A Novel Methodology for REDD+." *Carbon Balance and Management* 10 (1): 1–14. doi:10.1186/s13021-015-0023-8.
- Solberg, S., T.-P. Lohne, and O. Karyanto. 2015b. "Temporal Stability of InSAR Height in a Tropical Rainforest." *Remote Sensing Letters* 6 (3): 209–217. doi:10.1080/2150704X.2015.1026953.
- Solberg, S., E. Naeset, T. Gobakken, and O.-M. Bollandsås. 2014. "Forest Biomass Change Estimated from Height Change in Interferometric SAR Height Models." *Carbon Balance and Management* 9 (1): 1–12. doi:10.1186/s13021-014-0005-2.
- Solberg, S., D. J. Weydahl, and R. Astrup. 2015c. "Temporal Stability of X-Band Single-Pass InSAR Heights in a Spruce Forest: Effects of Acquisition Properties and Season." *IEEE Transactions on Geoscience and Remote Sensing* 53 (3): 1607–1614. doi:10.1109/TGRS.2014.2346473.
- Sorensen, K. W. 1993. "Indonesian Peat Swamp Forests and Their Role as a Carbon Sink." *Chemosphere* 27: 1065–1082. doi:10.1016/0045-6535(93)90068-G.
- St-Onge, B., Y. Hu, and C. Vega. 2008. "Mapping the Height and Above-Ground Biomass of a Mixed Forest Using Lidar and Stereo Ikonos Images." *International Journal of Remote Sensing* 29: 1277–1294. doi:10.1080/01431160701736505.
- Sweda, T., H. Tsuzuki, Y. Maeda, H.-D. V. Boehm, and S. H. Limin. 2012. "Above- and Below-Ground Carbon Budget of Degraded Tropical Peatland Revealed by Multi-temporal Airborne Laser Altimetry." In Proceedings of the 14th International Peat Congress.
- Treuhaft, R. N., B. D. Chapman, J. R. Dos Santos, F. G. Gonçalves, L. V. Dutra, P. M. L. A. Graça, and J. B. Drake. 2009. "Vegetation Profiles in Tropical Forests from Multibaseline Interferometric Synthetic Aperture Radar, Field, and Lidar Measurements." *Journal of Geophysical Research* 114: 1–16. doi:10.1029/2008JD011674.
- Treuhaft, R., F. Gonçalves, J. R. Dos Santos, M. Keller, M. Palace, S. N. Madsen, F. Sullivan, and P. M. L. A. Graça. 2015. "Tropical-Forest Biomass Estimation at X-Band From the Spaceborne TanDEM-X Interferometer." *IEEE Geoscience and Remote Sensing Letters* 12 (2): 239–243. doi:10.1109/LGRS.2014.2334140.
- Treuhaft, R. N., and P. R. Siqueira. 2004. "The Calculated Performance of Forest Structure and Biomass Estimates from Interferometric Radar." *Waves in Random Media* 14 (2): S345–358. doi:10.1088/0959-7174/14/2/013.
- Van der Werf, G. R., D. C. Morton, R. S. DeFries, J. G. J. Olivier, P. S. Kasibhatla, R. B. Jackson, G. J. Collatz, and J. T. Randerson. 2009. "CO₂ Emissions from Forest Loss." *Nature Geoscience* 2: 737–738. doi:10.1038/ngeo671.
- Verwer, C. C., and P. J. van der Meer. 2010. "Carbon Pools in Tropical Peat Forests – Towards a Reference Value for Forest Biomass Carbon in Relatively Undisturbed Peat Swamp Forests in Southeast Asia." Alterra-report 2108. Wageningen University and Research Center.
- Waldes, N. J. L., and S. E. Page. 2002. "Forest Structure and Tree Diversity of a Peat Swamp Forest in Central Kalimantan, Indonesia." Proceedings of International Symposium on Tropical Peatlands, 16–22.
- Wallington, E. D., and I. H. Woodhouse. 2004. "Forest Height Estimation from X-band SAR." *Proceedings of International Geoscience and Remote Sensing Symposium. IGARSS 2004*: 2393–2396.
- Wessel, B., T. Fritz, T. Busche, B. Bräutigam, G. Krieger, and M. Zink. 2013. "TanDEM-X Ground Segment." DEM Products Specification Document. Issue 3.0.
- Wessel, B., A. Gruber, M. Huber, M. Breunig, S. Wagenbrenner, A. Wendleder, and A. Roth. 2014. "Validation of the Absolute Height Accuracy of Tandem-X DEM for Moderate Terrain."

Proceedings of International Geoscience and Remote Sensing Symposium. IGARSS 2014: 3394–3397.

Weydahl, D. J., J. Sagstuen, Ø. B. Dick, and H. Rønning. 2007. "SRTM DEM Accuracy Assessment over Vegetated Areas in Norway." *International Journal of Remote Sensing* 28 (16): 3513–3527. doi:[10.1080/01431160600993447](https://doi.org/10.1080/01431160600993447).

Wösten, J. H. M., E. Clymans, S. E. Page, J. O. Rieley, and S. H. Limin. 2008. "Peat – Water Interrelationships in a Tropical Peatland Ecosystem in Southeast Asia." *Catena* 73: 212–224. doi:[10.1016/j.catena.2007.07.010](https://doi.org/10.1016/j.catena.2007.07.010).